HOKKAIDO UNIVERSITY

Title	Substituent Effects at the 5-Position of 3-[Bis(pyridine-2-ylmethyl)amino]-BODIPY Cation Sensor Used for Ratiometric Quantification of Cu2+
Author(s)	Hafuka, Akira; Kando, Ryosuke; Ohya, Kohei; Yamada, Koji; Okabe, Satoshi; Satoh, Hisashi
Citation	Bulletin of the Chemical Society of Japan, 88(3), 447-454 https://doi.org/10.1246/bcsj.20140273
Issue Date	2015-03-15
Doc URL	http://hdl.handle.net/2115/58602
Type	article (author version)
File Information	Hafuka 2015 BCSJ 88 447.pdf

Instructions for use

Hokkaido University Collection of Scholarly and Academic Papers : HUSCAP

Substituent effects at the 5-position of 3-[bis(pyridine-2-ylmethyl)amino]-BODIPY cation sensor used for ratiometric quantification of Cu^{2+}

Akira Hafuka*,[1] Ryosuke Kando,[2] Kohei Ohya,[2] Koji Yamada,[3] Satoshi Okabe,[2] and Hisashi Satoh[2]

[1] Department of Integrated Science and Engineering for Sustainable Society, Faculty of Science and Engineering, Chuo University, 1-13-27 Kasuga, Bunkyo-ku, Tokyo 112-8551, Japan

[2] Division of Environmental Engineering, Graduate School of Engineering, Hokkaido University, North-13, West-8, Sapporo 060-8628, Japan

[3] Division of Environmental Materials Science, Graduate School of Environmental Science, Hokkaido University, North-10, West-5, Sapporo 060-0810, Japan

Received Date: 11-Sep-2014

E-mail: hafuka.14p@g.chuo-u.ac.jp

In this paper, we investigated the effects of substitution at the 5-position of an asymmetric BODIPY cation sensor to tune its spectroscopic, photophysical, and cation-sensing properties. We introduced substituent groups with differing electron density at the 5-position of 3-[bis(pyridine-2-ylmethyl)amino]-BODIPY, which contains a cation recognition moiety at the 3-position of the BODIPY core, to develop four sensors which all exhibited distinctive ratiometric spectral changes in the presence of Cu^{2+}. Aromatic substitution increased the Stokes shift.

Substitution with the electron-withdrawing sulfonylphenyl group resulted in the highest fluorescence quantum yield, largest absorption coefficient, and largest spectral shift in the presence of Cu^{2+}. The sulfonylphenyl-substituted sensor also exhibited excellent selectivity for Cu^{2+}.

Copper (Cu) is a common heavy metal contaminant and it has toxic effects on aquatic organisms such as bacteria, plants, and fish.[1] Excess uptake of Cu^{2+} ion can cause diseases, such as Alzheimer's disease, Menkes disease, and Wilson disease.[2] Atomic absorption spectrometry (AAS) and inductively coupled plasma (ICP) spectroscopy are widely used for determination of heavy metals including Cu.[3] Although these instrumental analyses are precise, they are expensive and sometimes require complicated sample preparation. In addition, they are not employed for on-site monitoring and measure only the total concentration of heavy metals. Therefore, a cost-effective and simple analytical method is needed for determination of heavy metal ions.

Fluorescence spectroscopy is an attractive method for quantifying heavy metal ions due to its high sensitivity, operational simplicity, and versatile instrumentation.[4] Various fluorescent molecular sensors for Cu^{2+} have been reported.[5–9] However, most of reported fluorescent Cu^{2+} sensors exhibited fluorescence quenching because of paramagnetic property of Cu^{2+}. In terms of sensitivity, ratiometric fluorescent sensors are more favorable than those exhibiting only fluorescence quenching ("turn-off") or fluorescence enhancement ("turn-on"). [10]

BODIPY (4,4-difluoro-4-bora-3a,4a-diaza-*s*-indacene) derivatives show many characteristics useful for sensing, such as high molar absorption coefficient and fluorescence quantum yield, sharp

absorption and fluorescence bands, and good photochemical stability.[11–13] Furthermore, BODIPY derivatives can be excited with visible light (≥ 500 nm). The most distinctive feature of BODIPY derivatives is that their spectroscopic and photophysical properties can be tuned by appropriate substitution.[14] Among the eight positions of the BODIPY core, substitution of the 3- and 5-position(s) can significantly shift the absorption and fluorescence spectra.[14] Introducing a cation recognition moiety at the 3-position, and a substituent group at the 5-position of BODIPY, can create a ratiometric fluorescent cation sensor.[15–20] Methods for synthesizing these asymmetric BODIPY cation sensors include nucleophilic substitution of BODIPY chloride,[15, 18, 19, 21–24] condensation of 3,5-dimethyl-BODIPY with benzaldehyde,[16, 17] and palladium-catalyzed cross-coupling of BODIPY chloride.[20–22] Nucleophilic substitution of 3,5-dichloro-BODIPY is a practical synthetic method because commercially available (or easily synthesized) secondary amine can be easily introduced as a cation recognition moiety. In previous studies, a methoxy group has often been introduced at the 5-position of BODIPY by nucleophilic substitution.[15, 18, 19, 24] However, few studies have been conducted on substituent effects at the 5-position of asymmetric BODIPY cation sensors.[21, 22] The spectroscopic, photophysical, and cation-sensing properties of the BODIPY fluorescent sensors can depend not only on the cation recognition moiety at the 3-position, but also on the structure as a whole, including the substituent group at the 5-position. To improve the properties of BODIPY cation sensors and to investigate the effects of substitution at the 5-position, we have introduced four types of substituent groups to 5-position of 3-[bis(pyridine-2-ylmethyl)amino]-BODIPY (Scheme 1). We first introduce a substituent at the

5-position via Suzuki–Miyaura cross-coupling, where the substituent is one of three types that differ in electron density. We then introduce bis(pyridine-2-ylmethyl)amine [known as di(2-picolyl)amine: DPA] as the cation recognition moiety at the 3-position by aromatic nucleophilic substitution. We report herein the spectroscopic and photophysical properties, and cation sensing abilities, of the resulting sensors.

Results and discussion

Synthesis of BODIPY 1a–d

The chemical structures of BODIPY **1a–d** are shown in Figure 1. The first step uses the Suzuki–Miyaura cross-coupling reaction to introduce different aromatic groups (sulfonylphenyl, methoxyphenyl, or phenyl) at the 5-position.[14] The substituent groups differ in electron density. The sulfonylphenyl group is electron-withdrawing, while the methoxyphenyl group is electron-donating. We also prepared methoxy-substituted BODIPY, by using nucleophilic substitution, and then compared spectroscopic and photophysical properties of the four BODIPY derivatives. In the second step, we introduced DPA as the cation recognition moiety at the 3-position of each BODIPY by aromatic nucleophilic substitution.[25] This recognition moiety has an especially high affinity for Cu^{2+} and Zn^{2+}.[17, 19, 21–23, 26] 2,6-Dimethylphenyl group was introduced to 8-position of BODIPY core to increase fluorescence quantum yield by restricting internal rotation of the phenyl ring.[27] Table 1 shows the yield of the first and the second steps in the synthesis. The sulfonylphenyl-substituted BODIPY **1a** was obtained in good yield (75% in the first step and 80%

in the second step). Although di-substituted BODIPY was also obtained in the first step, mono-substituted compound **2a** was mainly obtained for 3h reaction time. Conversely, the methoxyphenyl-substituted BODIPY **1b** was obtained in relatively low yield (Table 1). Compared to the reaction to yield compound **2a**, a small amount of di-substituted BODIPY was obtained in the first step and the starting material compound **3** could be recovered after the reaction.[14] The yield of the subsequent aromatic nucleophilic substitution of bis(pyridine-2-ylmethyl)amine was high in the reaction to obtain BODIPY **1a**. Figure 2 shows the possible reaction mechanism for aromatic nucleophilic substitution of 5-aryl-BODIPY, where an electron-withdrawing sulfonylphenyl group at the 5-position may stabilize the carbanion intermediate and result in good yield.

Spectroscopic and photophysical properties of BODIPY 1a–d

Figure 3 shows the normalized absorption and fluorescence spectra of BODIPY **1a–d**. Methoxy-substituted BODIPY **1d** showed the longest absorption wavelength, at 534 nm. Because of extension of the π-conjugation, the fluorescence peak of the aromatic-substituted BODIPY **1a–c** occurred at a longer wavelength than that of **1d**. The fluorescence peak of the methoxyphenyl-substituted BODIPY **1b** occurred at the longest wavelength (599 nm).

Table 2 shows the spectroscopic and photophysical properties of BODIPY **1a–d**. All BODIPY derivatives had high fluorescence quantum yield, in the range of 0.58–0.63. Compared with methoxy-substituted BODIPY **1d**, aromatic-substituted BODIPY **1a–c** showed a higher molar

absorption coefficient (ε) in the visible range because of its extended π-conjugation. Among them, BODIPY **1c** exhibited the highest absorption coefficient (30,000 $M^{-1}cm^{-1}$). Additionally, BODIPY **1a–c** showed a larger Stokes shift (> 2,400 cm^{-1}) than that of BODIPY **1d**. These results indicate that aromatic substitution at the 5-position of 3-[bis(pyridine-2-ylmethyl)amino]-BODIPY increases the Stokes shift.[4, 10, 28]

Table 3 shows the spectroscopic and photophysical properties of BODIPY **1a–d** in the presence of Zn^{2+} (100 eq.). The zinc cation caused a blue-shift in both the absorption ($\Delta\lambda_{abs}$ = 28 nm) and fluorescence ($\Delta\lambda_{flu}$ = 24 nm) spectra of methoxy-substituted BODIPY **1d**. This spectral response can be explained by intramolecular charge transfer.[29] In contrast to BODIPY **1d**, in the presence of Zn^{2+} the absorption spectra of aromatic-substituted BODIPY **1a–c** shifted to the red ($\Delta\lambda_{abs}$ was about 35 nm), while their fluorescence spectra shifted to the blue ($\Delta\lambda_{flu}$ was about 10 nm). Furthermore, addition of Zn^{2+} increased the molar absorption coefficient of BODIPY **1a–c** and the fluorescence quantum yield of BODIPY **1a** and **1c**. The absorption and fluorescence of methoxyphenyl-substituted BODIPY **1b** was furthest to the red in the presence of Zn^{2+}, with an absorbance peak at 559 nm and a fluorescence peak at 590 nm.

Table 4 shows the spectroscopic and photophysical properties of BODIPY **1a–d** in the presence of Cu^{2+} (100 eq.). As is the case for Zn^{2+} addition, a blue-shift occurred in both the absorption ($\Delta\lambda_{abs}$ = 30 nm) and fluorescence ($\Delta\lambda_{flu}$ = 25 nm) spectra of methoxy-substituted BODIPY **1d** upon addition

of Cu^{2+}. In contrast, both the absorption and fluorescence spectra of aromatic-substituted BODIPY **1a–c** showed a red-shift upon the addition of Cu^{2+}. The red-shift in the fluorescence spectra of **1a–c** differs from their fluorescence response to Zn^{2+}, which manifests in a blue-shift. The extent of the shift in the absorption spectra of **1a–c** was around 80 nm, and that of their fluorescence spectra was around 40 nm. Methoxyphenyl-substituted BODIPY **1b** showed the longest-wavelength absorption (604 nm) and fluorescence (647 nm) in the presence of Cu^{2+}. However, **1b** and **1c** showed relatively low fluorescence quantum yield (Φ = 0.03 and 0.16, respectively) in the presence of Cu^{2+}, owing to the ability of Cu^{2+} to quench fluorescence. Among BODIPY **1a–d**, sulfonylphenyl-substituted BODIPY **1a** showed relatively high fluorescence quantum yield (Φ = 0.28) and large absorption coefficient (ε = 47,000 M^{-1} cm^{-1}). These results could indicate that the electron-withdrawing sulfonylphenyl group at the 5-position of 3-[bis(pyridine-2-ylmethyl)amino]-BODIPY reduced the quenching effect of Cu^{2+}.

Ratiometric sensing of Cu^{2+} with BODIPY 1a

Because BODIPY **1a** showed the largest fluorescence quantum yield, absorption coefficient, and spectral shift in the presence of Cu^{2+}, we further investigated its performance as a Cu^{2+} sensor. Figure 4 shows the influence of Cu^{2+} on the absorption and fluorescence spectra of BODIPY **1a.** With increasing Cu^{2+} concentration (0–10 μM), the original absorption band around 502 nm gradually decreases, while a new absorption peak at 590 nm appears and increases. Similar changes are observed in the fluorescence spectra, where the fluorescence peak at 581 nm (F_{581}) gradually

decreases while another peak at 620 nm (F_{620}) increases.

The fluorescence spectral change in BODIPY **1a**, shown in Figure 4b, enables Cu^{2+} concentration to be determined from the ratio of fluorescence intensities at 620 nm and at 581 nm (F_{620}/ F_{581}). Ratiometric fluorescent sensors are more favorable for quantitative measurement than those exhibiting only fluorescence enhancement ("turn-on") or fluorescence quenching ("turn-off").[10] Figure 5a shows that the ratio (F_{620}/ F_{581}) increases with increasing Cu^{2+} concentration. Based on the slope of the ratio (F_{620}/ F_{581}) in Cu^{2+} concentration range of 0–4 μM, the detection limit was determined as 3.2×10^{-7} M. By using a Benesi–Hildebrand plot (Figure 5b), the dissociation constant (K_d) of the complex between BODIPY **1a** and Cu^{2+} was found to be 3.82×10^{-6} M.[30]

To assess the selectivity of BODIPY **1a** for Cu^{2+}, the effect of other metal cations on the fluorescence intensity of BODIPY **1a** was investigated. Alkali and alkaline-earth metal ions (e.g. Na^{+}, Mg^{2+}, K^{+}, and Ca^{2+}) did not influence the fluorescence spectra of BODIPY **1a** (See Supplementary Data). As shown in Figure 6, no cations except Cu^{2+} influenced the F_{620}/F_{581} ratio of BODIPY **1a**. The white bars in Figure 6 represent the F_{620}/F_{581} upon addition of the other cations; in all cases the F_{620}/F_{581} remained less than 1. Subsequent addition of Cu^{2+} to the solutions significantly increased the F_{620}/F_{581} ratio to around 18, as shown by the black bars in Figure 6. Furthermore, the fluorescence and absorption spectra of the resulting samples overlapped those of the BODIPY **1a** samples to which only Cu^{2+} had been added. This result indicates that BODIPY **1a**

has good selectivity for Cu^{2+}.

Conclusions

The present study describes the design, synthesis, and testing of four asymmetric BODIPY cation sensors based on 3-[bis(pyridine-2-ylmethyl)amino]-BODIPY, whose substituent groups at the 5-position differed in electron density. The samples were evaluated for their response to Cu^{2+}. Aromatic substitution increased the Stokes shift of all the BODIPY samples. Among BODIPY **1a–d**, sulfonylphenyl-substituted BODIPY **1a** showed the highest fluorescence quantum yield, largest absorption coefficient, and largest red-shift in both the fluorescence and absorption spectra in response to Cu^{2+}. These results could indicate that the electron-withdrawing group at the 5-position prevented the quenching effect of Cu^{2+}. BODIPY **1a** furthermore showed good selectivity for Cu^{2+} and exhibited ratiometric spectral change in both the absorption and fluorescence spectra depending on Cu^{2+} concentration.

Experimental section

Materials and measurements

Unless otherwise stated, all reagents were purchased from commercial suppliers (Sigma-Aldrich, Wako Pure Chemical Industries, or Tokyo Chemical Industry) and used without further purification. ^{1}H and ^{13}C NMR spectra were recorded on a JEOL 400 (400 MHz ^{1}H; 100 MHz ^{13}C) spectrometer at room temperature. High resolution mass spectra (HRMS) were measured on a Thermo Scientific

Exactive or JEOL JMS-T100GCv mass spectrometer. Fluorescence spectra were obtained on a JASCO FP-6600 spectrofluorometer and absorption spectra were obtained on a JASCO V-630 spectrophotometer.

Synthesis

The synthetic route of BODIPY **1a–d** is shown in Scheme 1. Reactions were monitored using high-performance thin-layer chromatography (HPTLC; silica gel 60 F_{254}, Merck, Germany) or thin-layer chromatography (aluminum oxide 60 F_{254}, basic, Merck, Germany). HPTLC plates were visualized in ultraviolet light and/or by staining with anisaldehyde solution (anisaldehyde/ethanol/sulfuric acid/acetic acid = 1.9/68/2.5/1.2, v/v) followed by heating for a few minutes. Open-column chromatography was performed using silica gel 60 (230–400 mesh) or aluminum oxide 90 active basic (Merck, Germany). Chemical shifts in the NMR spectra are reported in ppm relative to tetramethylsilane as the internal standard (residual $CHCl_3$; ^{1}H NMR 7.26 ppm, ^{13}C NMR 77.2 ppm). Coupling constants (*J*) are reported in hertz. Splitting patterns are indicated as s, singlet; d, doublet; t, triplet; q, quartet; m, multiplet; brs, broad singlet for ^{1}H NMR data.

Synthesis of 4-(5,5-dimethyl-1,3,2-dioxaborolan-2-yl)benzenesulfonic acid 2,2-dimethylpropyl ester (7)

4-Bromobenzenesulfonic acid 2,2-dimethylpropyl ester (520 mg, 1.69 mmol, 1 equiv.),

bis-(neopentyl glycolato)-diboron (460 mg, 2.03 mmol, 1.2 equiv.), potassium acetate (500 mg, 5.08 mmol, 3 equiv.), and [1,1′-bis(diphenylphosphino)ferrocene]palladium dichloride dichloromethane adduct (41 mg, 3 mol %) were dissolved in dimethyl sulfoxide (10 mL). The reaction mixture was stirred at 90 °C for 1 h. After being cooled to room temperature, chloroform was added to the mixture, and the organic layer was washed with water and brine. The organic layer was dried over Na_2SO_4. The solvent was evaporated and the crude product was purified by column chromatography on silica gel (hexane/ethyl acetate = 5/1) to yield compound **7** (404 mg, 70%) as a white solid. ^{1}H NMR (400 MHz, $CDCl_3$): δ = 7.96 (d, 2H, J = 8.4 Hz), 7.86 (d, 2H, J = 8.5 Hz), 3.79 (s, 4H), 3.65 (s, 2H), 1.04 (s, 6H), 0.88 (9H); ^{13}C NMR (100 MHz, $CDCl_3$): δ = 134.3, 126.6, 79.6, 72.4, 31.9, 31.6, 26.0, 21.8; HRMS (FD): *m/z* calcd for $C_{16}H_{25}BO_5S$: 339.1552 $[M]^+$; found: 339.1549.

*Synthesis of compound **6***

5-(2,6-Dimethylphenyl)dipyrromethane (6): 2,6-Dimethylbenzaldehyde (3.8 g, 29.0 mmol, 1 equiv.) was added to a two-necked flask under nitrogen. The flask was heated to 40 °C, following which pyrrole (80 mL, 1.16 mol, 40 equiv.) was added to the solution with stirring. After being stirred for 10 min, trifluoroacetic acid (230 μL, 2.90 mmol, 0.1 equiv.) was added to the solution and the reaction mixture was stirred at 40 °C for 30 min. The solution was then cooled to room temperature, after which dichloromethane was added and the mixture was washed with water, followed by washing with saturated aqueous sodium bicarbonate. The organic layer was washed

with brine and dried over Na_2SO_4. The solvent was evaporated and the crude product was purified by column chromatography on silica gel (hexane/ethyl acetate = 5/1) to yield compound **6** (6.5 g, 91%) as a black solid. ^{1}H NMR (400 MHz, $CDCl_3$): δ = 7.94 (br, 2H), 7.13–7.09 (m, 1H), 7.04 (d, 2H, *J* = 7.5 Hz), 6.68–6.67 (m, 2H), 6.18 (q, 2H, *J* = 2.9 Hz), 6.01–5.99 (m, 2H), 5.97 (s, 1H), 2.10 (s, 6H); ^{13}C NMR (100 MHz, $CDCl_3$): δ = 137.6, 130.8, 129.4, 127.0, 116.1, 108.5, 106.5, 38.6, 20.6; HRMS (ESI): *m/z* calcd for $C_{17}H_{18}N_2H$: 251.1543$[M+H]^+$; found: 251.1542.

*Synthesis of compound **5***

1,9-Dichloro-5-(2,6-dimethylphenyl)dipyrromethane (5): Compound **6** (1.0 g, 3.99 mmol, 1 equiv.) was dissolved in dry tetrahydrofuran (40 mL) under nitrogen. The solution was cooled to −78 °C. A suspension of *N*-chlorosuccinimide (1.1 g, 8.39 mmol, 2.1 equiv.) in tetrahydrofuran (20 mL) was then added to the solution with stirring. After the reaction mixture had been stirred at −78 °C for 5 h, water was added and the mixture was extracted with dichloromethane. The organic layer was washed with brine and dried over Na_2SO_4. The solvent was evaporated and the crude product was purified by column chromatography on silica gel (hexane/ethyl acetate = 15/1) to yield compound **5** (1.2 g, 95%) as a black solid. ^{1}H NMR (400 MHz, $CDCl_3$): δ = 7.75 (br, 2H), 7.16–7.12 (m, 1H), 7.06 (d, 2H, *J* = 7.6 Hz), 5.99–5.97 (m, 2H), 5.91–5.89 (m, 2H), 5.79 (s, 1H), 2.14 (s, 6H); ^{13}C NMR (100 MHz, $CDCl_3$): δ = 137.5, 135.9, 129.6, 129.5, 127.4, 112.6, 107.8, 106.4, 38.7, 20.7; HRMS (ESI): *m/z* calcd for $C_{17}H_{15}Cl_2N_2$: 317.0618 $[M]^+$; found: 317.0619.

*Synthesis of compound **4***

1,9-Dichloro-5-(2,6-dimethylphenyl)dipyrromethene (4): Compound **5** (960 mg, 3.01 mmol, 1 equiv.) was dissolved in dichloromethane (80 mL). A suspension of *p*-chloranil (813 mg, 3.31 mmol, 1.1 equiv.) in dichloromethane (20 mL) was then added to the solution with stirring. After being stirred at room temperature for 2 h, the solvent was evaporated and the crude product was purified by column chromatography on silica gel (hexane/ethyl acetate = 20/1) to yield compound **4** (742 mg, 78%) as a black solid. ^{1}H NMR (400 MHz, $CDCl_3$): δ = 7.23 (t, 1H, J = 7.6 Hz), 7.09 (d, 2H, J = 7.6 Hz), 6.30 (d, 2H, J = 4.3 Hz), 6.19 (d, 2H, J = 4.2 Hz), 2.11 (s, 6H); ^{13}C NMR (100 MHz, $CDCl_3$): δ = 141.2, 138.3, 138.0, 136.9, 134.2, 128.4, 128.2, 127.0, 117.0, 19.9; HRMS (ESI): *m/z* calcd for $C_{17}H_{14}Cl_2N_2H$: 317.0607 $[M+H]^+$; found: 317.0610.

*Synthesis of compound **3***

3,5-Dichloro-4,4-difluoro-8-(2,6-dimethylphenyl)-4-bora-3a,4a-diaza-*s*-indacene (3): Compound **4** (740 mg, 2.33 mmol, 1 equiv.) was dissolved in dry toluene (80 mL) under nitrogen. Triethylamine (3.2 mL, 23.3 mmol, 10 equiv.) was then added to the solution. After being stirred at 70 °C for 30 min, $BF_3{\cdot}Et_2O$ (4.4 mL, 35.0 mmol, 15 equiv.) was added dropwise to the solution and the reaction mixture was gradually heated and refluxed for 2 h. After being cooled to room temperature, dichloromethane was added and the mixture was washed with water, saturated aqueous sodium bicarbonate, and brine. The organic layer was dried over Na_2SO_4. The solvent was evaporated and the crude product was purified by column chromatography on silica gel

(hexane/ethyl acetate = 20/1) to yield compound **3** (637 mg, 75%) as a dark brown solid. ^{1}H NMR (400 MHz, $CDCl_3$): δ = 7.29 (t, 1H, *J* = 7.6 Hz), 7.13 (d, 2H, *J* = 7.8 Hz), 6.59 (d, 2H, *J* = 4.2 Hz), 6.37 (d, 2H, *J* = 4.2 Hz), 2.14 (s, 6H); ^{13}C NMR (100 MHz, $CDCl_3$): δ = 144.9, 143.4, 136.6, 133.7, 130.9, 130.0, 129.2, 127.4, 118.9, 20.0; HRMS (ESI): *m/z* calcd for $C_{17}H_{13}BCl_2F_2N_2$: 363.0559 $[M]^+$; found: 363.0569.

*General procedure for the synthesis of 5-subtituted-BODIPYs **2a–c***

Compound **3** (1 equiv.), aryl boronic acid or aryl boronic ester (1.2 equiv.), cesium fluoride (3 equiv.), and tetrakis (triphenylphosphine) palladium (5 mol %) were dissolved in dry toluene. The reaction mixture was stirred with heating under nitrogen. After being cooled to room temperature, water was added to the mixture and the organic layer was extracted with dichloromethane. The combined organic layers were washed with brine and then dried over Na_2SO_4. The solvent was evaporated and the crude product was purified by column chromatography.

3-Chloro-4,4-difluoro-5-[4-(2,2-dimethyl-propoxysulfonyl)phenyl]-8-(2,6-dimethylphenyl)-4-bora-3a,4a-diaza-*s*-indacene (2a): Compound **7** was used as the boronic ester. The reaction mixture was stirred at 60 °C for 3 h. The crude product was purified by column chromatography on silica gel (hexane/ethyl acetate = 5/1) to yield compound **2a** (75%) as a dark red solid. ^{1}H NMR (400 MHz, $CDCl_3$): δ = 8.13 (d, 2H, *J* = 8.4 Hz), 8.00 (d, 2H, *J* = 8.3 Hz), 7.32 (t, 1H, *J* = 7.6 Hz), 7.17 (d, 2H, *J* = 7.6 Hz), 6.71 (d, 2H, *J* = 4.3 Hz), 6.66–6.64 (m, 2H), 6.40 (d, 2H, *J* = 4.3 Hz), 3.77 (s, 2H), 2.19 (s, 6H), 0.94 (s, 9H); ^{13}C NMR (100 MHz, $CDCl_3$): δ = 144.1, 137.0, 136.6, 136.5, 131.6,

130.2, 130.1, 130.0, 129.9, 129.9, 129.2, 128.5, 128.0, 127.7, 127.4, 121.0, 119.3, 79.9, 79.8, 31.7, 26.0, 20.1; HRMS (ESI): *m/z* calcd for $C_{28}H_{28}BClF_2N_2O_3S$: 555.1612 $[M]^+$; found: 555.1624.

3-Chloro-4,4-difluoro-5-(4-methoxyphenyl)-8-(2,6-dimethylphenyl)-4-bora-3a,4a-diaza-*s*-indacene (2b): 4-Methoxyphenyl boronic acid was used as the boronic acid. The reaction mixture was stirred at 80 °C for 3 h. The crude product was purified by column chromatography on silica gel (hexane/ethyl acetate = 1/2) to yield compound **2b** (15%) as a dark red solid. ^{1}H NMR (400 MHz, $CDCl_3$): δ = 8.01 (d, 2H, *J* = 8.6 Hz), 7.29 (t, 1H, *J* = 7.6 Hz), 7.14 (d, 2H, *J* = 7.5 Hz), 7.02 (d, 2H, *J* = 8.6 Hz), 6.68–6.65 (m, 2H), 6.47 (d, 1H, *J* = 4.0 Hz), 6.30 (d, 1H, *J* = 4.1 Hz), 3.89 (s, 3H), 2.18 (s, 6H); ^{13}C NMR (100 MHz, $CDCl_3$): δ = 161.3, 141.8, 136.8, 132.1, 131.3, 131.3, 131.2, 131.2, 128.8, 127.6, 127.2, 126.9, 124.1, 121.6, 117.2, 113.9, 55.3, 29.7, 20.1; HRMS (ESI): *m/z* calcd for $C_{24}H_{20}BClF_2N_2ONa$: 458.1254 $[M+Na]^+$; found: 458.1263.

3-Chloro-4,4-difluoro-5-phenyl-8-(2,6-dimethylphenyl)-4-bora-3a,4a-diaza-*s*-indacene (2c): 5,5-Dimethyl-2-phenyl-1,3,2-dioxaborinane was used as the boronic ester. The reaction mixture was stirred at 80 °C for 3 h. The crude product was purified by column chromatography on silica gel (toluene). The obtained crude red solid was used for the subsequent preparation. HRMS (ESI): *m/z* calcd for $C_{23}H_{18}BClF_2N_2Na$: 428.1148 $[M+Na]^+$; found: 428.1145.

*Synthesis of 5-subtituted-BODIPY **2d***

3-Chloro-4,4-difluoro-5-methoxy-8-(2,6-dimethylphenyl)-4-bora-3a,4a-diaza-*s*-indacene (2d): Compound **3** (50 mg, 0.14 mmol, 1 equiv.) was dissolved in absolute methanol (15 mL) under

nitrogen. Sodium methoxide (7.4 mg, 0.14 mmol, 1 equiv.) in methanol (5 mL) was added dropwise with stirring. The reaction mixture was stirred at room temperature for 30 min. The reaction was quenched with water and extracted with dichloromethane. The combined organic layers were washed with brine and then dried over Na_2SO_4. The solvent was evaporated and the crude product was purified by column chromatography on silica gel (hexane/ethyl acetate = 4/1) to yield compound **2d** (48 mg, 96%) as a dark red solid. ^{1}H NMR (400 MHz, $CDCl_3$): δ = 7.26 (t, 1H, J = 7.6 Hz), 7.11 (d, 2H, J = 7.5 Hz), 6.70 (d, 1H, J = 4.6 Hz), 6.31 (d, 1H, J = 3.9 Hz), 6.21 (d, 1H, J = 4.0 Hz), 6.12 (d, 1H, J = 4.7 Hz), 4.15 (s, 3H), 2.12 (s, 6H); ^{13}C NMR (100 MHz, $CDCl_3$): δ = 169.4, 139.3, 136.9, 136.8, 133.7, 131.8, 131.5, 130.1, 128.8, 127.2, 124.6, 115.4, 104.8, 60.3, 59.2, 21.0, 19.9, 14.2; HRMS (ESI): *m/z* calcd for $C_{18}H_{16}BClF_2N_2ONa$: 382.0941 $[M+Na]^+$; found: 382.0946.

*General procedure for the synthesis of BODIPY **1a–d***

5-substituted BODIPY (1 equiv.) was dissolved in acetonitrile. Di(2-picolyl)amine (1.5 equiv.) and triethylamine (30 equiv.) were then added to the solution. The reaction mixture was refluxed with stirring under nitrogen. After being cooled to room temperature, ethyl acetate was added and the mixture was washed with water and brine. The organic layer was dried over Na_2SO_4, the solvent was evaporated, and the crude product was purified by column chromatography.

3-[Bis(pyridine-2-ylmethyl)amino]-4,4-difluoro-5-[4-(2,2-dimethyl-propoxysulfonyl)phenyl]-8-(2,6-dimethylphenyl)-4-bora-3a,4a-diaza-*s*-indacene (1a): The reaction mixture was stirred for 3

h. The crude product was purified by column chromatography on aluminum oxide basic (hexane/ethyl acetate = 3/1) to yield compound **1a** (80%) as a dark pink solid. ^{1}H NMR (400 MHz, $CDCl_3$): δ = 8.55–8.53 (m, 2H), 8.01 (d, 2H, *J* = 8.8 Hz), 7.85 (d, 2H, *J* = 8.7 Hz), 7.65 (td, 2H, *J* = 7.7, 1.8 Hz), 7.33 (d, 2H, *J* = 7.9 Hz), 7.24 (t, 1H, *J* = 7.6 Hz), 7.20–7.17 (m, 2H), 7.11 (d, 2H, *J* = 7.5 Hz), 6.58 (d, 2H, *J* = 5.1 Hz), 6.45 (d, 2H, *J* = 3.8 Hz), 6.30 (d, 2H, *J* = 5.1 Hz), 6.15 (d, 2H, *J* = 3.9 Hz), 5.21 (s, 4H), 3.69 (s, 2H), 2.18 (s, 6H), 0.88 (s, 9H); ^{13}C NMR (100 MHz, $CDCl_3$): δ = 163.8, 155.9, 149.3, 144.3, 139.8, 137.4, 136.7, 135.2, 134.0, 133.7, 133.4, 133.4, 131.0, 129.2, 128.2, 127.2, 127.1, 122.5, 121.8, 118.7, 116.6, 115.9, 79.5, 57.7, 31.6, 26.0, 20.1; HRMS (ESI): *m/z* calcd for $C_{40}H_{40}BF_2N_5O_3SH$: 719.3022 $[M+H]^+$; found: 719.3032.

3-[Bis(pyridine-2-ylmethyl)amino]-4,4-difluoro-5-(4-methoxyphenyl)-8-(2,6-dimethylphenyl)-4-bora-3a,4a-diaza-*s*-indacene (1b): The reaction mixture was stirred for 3 h. The crude product was purified by column chromatography on aluminum oxide basic (hexane/ethyl acetate = 1/2) to yield compound **1b** (10%) as a dark pink solid. ^{1}H NMR (400 MHz, $CDCl_3$): δ = 8.52 (d, 2H, *J* = 4.8 Hz), 7.81 (d, 2H, *J* = 8.8 Hz), 7.63 (td, 2H, *J* = 7.7, 1.8 Hz), 7.38 (d, 2H, *J* = 7.9 Hz), 7.22 (t, 1H, *J* = 7.5 Hz), 7.18–7.15 (m, 2H), 7.10 (d, 2H, *J* = 7.6 Hz), 6.91 (d, 2H, *J* = 8.8 Hz), 6.50 (d, 1H, *J* = 5.0 Hz), 6.34 (d, 1H, *J* = 3.8 Hz), 6.18 (d, 1H, *J* = 3.8 Hz), 6.14 (d, 1H, *J* = 5.0 Hz), 5.17 (s, 4H), 3.83 (s, 3H), 2.19 (s, 6H); ^{13}C NMR (100 MHz, $CDCl_3$): δ = 159.0, 156.6, 149.2, 137.4, 136.7, 133.7, 132.6, 130.2, 128.0, 127.0, 126.9, 122.3, 121.9, 120.2, 116.1, 113.8, 113.2, 68.1, 57.8, 55.1, 38.7, 30.3, 28.9, 20.1, 11.0; HRMS (ESI): *m/z* calcd for $C_{36}H_{32}BF_2N_5ONa$: 621.2597 $[M+Na]^+$; found: 621.2595.

3-[Bis(pyridine-2-ylmethyl)amino]-4,4-difluoro-5-phenyl-8-(2,6-dimethylphenyl)-4-bora-3a,4a-diaza-*s*-indacene (1c): The reaction mixture was stirred for 1 h. The crude product was purified by column chromatography on silica gel (chloroform/methanol = 10/1) to yield compound **1c** (12% in two steps) as a dark pink solid. ^{1}H NMR (400 MHz, $CDCl_3$): δ = 8.51 (d, 2H, *J* = 4.9 Hz), 7.85 (d, 2H, *J* = 8.3 Hz), 7.62 (td, 2H, *J* = 7.7, 1.8 Hz), 7.39–7.35 (m, 4H), 7.30 (t, 1H, *J* = 7.3 Hz), 7.24–7.21 (m, 1H), 7.18–7.14 (m, 2H), 7.10 (d, 2H, *J* = 7.5 Hz), 6.52 (d, 1H, *J* = 5.0 Hz), 6.37 (d, 1H, *J* = 3.8 Hz), 6.18–6.17 (m, 2H), 5.17 (s, 4H), 2.19 (s, 6H); ^{13}C NMR (100 MHz, $CDCl_3$): δ = 163.0, 156.4, 149.2, 148.3, 137.4, 136.7, 134.4, 133.7, 132.9, 131.9, 129.0, 128.9, 128.1, 127.6, 127.3, 127.0, 125.1, 12.4, 121.9, 119.8, 116.2, 114.3, 57.7, 20.1; HRMS (ESI): *m/z* calcd for $C_{35}H_{30}BF_2N_5Na$: 591.2491 $[M+Na]^+$; found: 591.2487.

3-[Bis(pyridine-2-ylmethyl)amino]-4,4-difluoro-5-methoxy-8-(2,6-dimethylphenyl)-4-bora-3a,4a-diaza-*s*-indacene (1d): The reaction mixture was stirred for 3 h. The crude product was purified by column chromatography on basic aluminum oxide (hexane/ethyl acetate = 1/4) to yield compound **1d** (24%) as a dark pink solid. ^{1}H NMR (400 MHz, $CDCl_3$): δ = 8.52 (d, 2H, *J* = 4.8 Hz), 7.65 (td, 2H, *J* = 7.7, 1.8 Hz), 7.46 (d, 2H, *J* = 7.9 Hz), 7.20 (t, 1H, *J* = 7.6 Hz), 7.17–7.14 (m, 2H), 7.07 (d, 2H, *J* = 7.6 Hz), 6.40 (d, 1H, *J* = 4.8 Hz), 6.17 (d, 1H, *J* = 4.1 Hz), 6.02 (d, 1H, *J* = 4.8 Hz), 5.66 (d, 1H, *J* = 4.2 Hz), 5.13 (s, 4H), 3.98 (s, 3H), 2.15 (s, 6H); ^{13}C NMR (100 MHz, $CDCl_3$): δ = 161.6, 157.0, 149.1, 137.5, 136.7, 133.1, 132.5, 131.2, 128.0, 126.9, 122.2, 121.9, 111.4, 95.0, 58.1, 57.7, 29.7, 19.9; HRMS (ESI): *m/z* calcd for $C_{30}H_{28}BF_2N_5OH$: 523.2464 $[M+H]^+$; found: 523.2475.

Analytical procedure

All spectroscopic measurements were carried out in analytical grade acetonitrile. Stock solutions of BODIPY **1a–d** (50 μM) were prepared by dissolving each BODIPY in acetonitrile, while stock solutions of metal ion (200 μM) were prepared by dissolving appropriate amounts of perchlorate salts in acetonitrile. Each test solution was prepared by adding an aliquot (400 μL) of the BODIPY and the metal ion stock solution (20–1000 μL) into a 10 mL volumetric flask by using a micropipette, then diluting the solution with acetonitrile. Quartz cells with a cross section of 1 cm × 1 cm were used for measurements of absorption and fluorescence spectra. In the absorbance determination, an appropriate volume of the metal ion stock solution was spiked into a reference cell to ensure the absorbance of the test sample. The dissociation constant (K_d) between BODIPY **1a** and Cu^{2+} was evaluated by using a Benesi–Hildebrand plot.[31] The K_d value can be calculated by dividing the slope by the intercept. The excitation slit width was 5.0 nm and the emission slit width was 6.0 nm. The detection limit (LOD, 3σ/slope) for Cu^{2+} was determined based on the standard deviation (σ) in the fluorescence intensity of 11 blank solutions.[32] The fluorescence quantum yields were obtained by comparing the area under the corrected fluorescence spectrum of the test sample with that of a solution of Rhodamine 6G in ethanol, which has a reported quantum yield (Φ_R) of 0.95.[33] The quantum yield of fluorescence (Φ_S) for each sample was obtained from multiple measurements (N = 3) using the following Equation 1:

$$\Phi_S = \Phi_R \times S_S/S_R \times A_R/A_S \times (\eta_S/\eta_R)^2 \qquad (1)$$

where Φ is the quantum yield, S is the integrated area of the corresponding fluorescence spectrum,

A is the absorbance at the excitation wavelength, η is the refractive index of the solvent used, and S and R refer to the sample and the reference fluorophore, respectively. All reported data are the average of at least three replicates.

This research was financially supported by Grants-in-Aid for Scientific Research (No. 12J01817, No. 23686074, and No. 26289178) from the Japan Society for the Promotion of Science. The authors especially thank Mr. Hiroaki Yoshikawa and Mr. Akiyoshi Takitani for experimental support.

Supporting Information

Supporting information is available.

References

1 A. Johnson, E. Carew, K. A. Sloman, *Aquat. Toxicol.* **2007**, *84*, 431.

2 D. J. Waggoner, T. B. Bartnikas, J. D. Gitlin, *Neurobiol. Dis.* **1999**, *6*, 221.

3 *Standard Methods for the Examination of Water and Wastewater,* 22nd ed., American Public Health Association, Washington, **2012**.

4 *Principles of Fluorescence Spectroscopy*, 3rd ed., ed. by J. R. Lakowicz, Springer, New York, **2006**.

5 Z. P. Liu, C. L. Zhang, X. Q. Wang, W. J. He, Z. J. Guo, *Org. Lett.* **2012**, *14*, 4378.

6 J. G. Huang, M. Liu, X. Q. Ma, Q. Dong, B. Ye, W. Wang, W. B. Zeng, *RSC Adv.* **2014**, *4*, 22964.

7 M. Li, H. B. Ge, R. L. Arrowsmith, V. Mirabello, S. W. Botchway, W. H. Zhu, S. I. Pascu, T. D. James, *Chem. Commun.* **2014**, *50*, 11806.

8 Y. F. Wang, L. Zhang, G. J. Zhang, Y. Wu, S. Y. Wu, J. J. Yu, L. M. Wang, *Tetrahedron Lett.* **2014**, *55*, 3218.

9 J. T. Yeh, W. C. Chen, S. R. Liu, S. P. Wu, *New J. Chem.* **2014**, *38*, 4434.

10 B. Valeur, *Molecular Fluorescence: Principles and Applications*, 2nd ed., Wiley-VCH, Weinheim, **2012**.

11 A. Loudet, K. Burgess, *Chem. Rev.* **2007**, *107*, 4891.

12 G. Ulrich, R. Ziessel, A. Harriman, *Angew. Chem. Int. Edit.* **2008**, *47*, 1184.

13 N. Boens, V. Leen, W. Dehaen, *Chem. Soc. Rev.* **2012**, *41*, 1130.

14 T. Rohand, W. Qin, N. Boens, W. Dehaen, *Eur. J. Org. Chem.* **2006**, *20*, 4658.

15 M. Baruah, W. Qin, R. A. L. Vallee, D. Beljonne, T. Rohand, W. Dehaen, N. Boens, *Org. Lett.* **2005**, *7*, 4377.

16 X. Peng, J. Du, J. Fan, J. Wang, Y. Wu, J. Zhao, S. Sun, T. Xu, *J. Am. Chem. Soc.* **2007**, *129*, 1500.

17 S. Atilgan, T. Ozdemir, E. U. Akkaya, *Org. Lett.* **2008**, *10*, 4065.

18 D. W. Domaille, L. Zeng, C. J. Chang, *J. Am. Chem. Soc.* **2010**, *132*, 1194.

19 J. L. Huang, B. Wang, J. G. Ye, B. Liu, H. Y. Qiu, S. C. Yin, *Chin. J. Chem.* **2012**, *30*, 1857.

20 A. Hafuka, H. Taniyama, S. H. Son, K. Yamada, M. Takahashi, S. Okabe, H. Satoh, *Bull. Chem. Soc. Jpn.* **2013**, *86*, 37.

21 S. Yin, V. Leen, S. Van Snick, N. Boens, W. Dehaen, *Chem. Commun.* **2010**, *46*, 6329.

22 S. C. Yin, W. L. Yuan, J. L. Huang, D. B. Xie, B. Liu, K. Z. Jiang, H. Y. Qiu, *Spectroc. Acta Pt. A-Molec. Biomolec. Spectr.* **2012**, *96*, 82.

23 X. Jia, X. T. Yu, G. L. Zhang, W. S. Liu, W. W. Qin, *J. Coord. Chem.* **2013**, *66*, 662.

24 I. Moczar, P. Huszthy, Z. Maidics, M. Kadar, K. Toth, *Tetrahedron*. **2009**, *65*, 8250.

25 T. Rohand, M. Baruah, W. W. Qin, N. Boens, W. Dehaen, *Chem. Commun.* **2010**, 266.

26 S. C. Burdette, G. K. Walkup, B. Spingler, R. Y. Tsien, S. J. Lippard, *J. Am. Chem. Soc.* **2001**, *123*, 7831.

27 K. Yamada, T. Toyota, K. Takakura, M. Ishimaru, T. Sugawara, *New J. Chem.* **2001**, *25*, 667.

28 Y. H. Chen, J. Z. Zhao, H. M. Guo, L. J. Xie, *J. Org. Chem.* **2012**, *77*, 2192.

29 B. Valeur, I. Leray, Coordin. *Chem. Rev.* **2000**, *205*, 3.

30 H. X. Wang, L. Yang, W. B. Zhang, Y. Zhou, B. Zhao, X. Y. Li, *Inorg. Chim. Acta*. **2012**, *381*, 111.

31 K. A. Connars, *Binding Constants*, Wiley-Interscience, New York, **1987**.

32 Z. X. Han, X. B. Zhang, L. Zhuo, Y. J. Gong, X. Y. Wu, J. Zhen, C. M. He, L. X. Jian, Z. Jing, G. L. Shen, R. Q. Yu, *Anal. Chem.* **2010**, *82*, 3108.

33 D. Magde, R. Wong, P. G. Seybold, *Photochem. Photobiol.* **2002**, *75*, 327.

Table 1. Synthetic yields (%) of BODIPY **1a–d**.

[a] The crude solid obtained in the 1st step was used for the subsequent 2nd step because we could not separate monophenyl- and diphenyl-substituted BODIPY.

Table 2. Spectroscopic and photophysical properties of BODIPY **1a–d** in acetonitrile.

Table 3. Spectroscopic and photophysical properties of BODIPY **1a–d** (2 μM) with Zn^{2+} (200 μM) in acetonitrile. $\Delta\lambda$ is the extent of the shift in wavelength caused by the addition of Zn^{2+}.

Table 4. Spectroscopic and photophysical properties of BODIPY **1a–d** (2 μM) with Cu^{2+} (200 μM) in acetonitrile. $\Delta\lambda$ is the extent of the shift in wavelength caused by the addition of Cu^{2+}.

Scheme 1. Synthesis of BODIPY **1a–d**.

Figure 1. Synthetic route and the chemical structures of BODIPY **1a–d**.

Figure 2. Possible reaction mechanism for the aromatic nucleophilic substitution of 5-aryl-BODIPY.

Figure 3. Normalized absorption (a) and fluorescence (b) spectra of BODIPY **1a–d** in acetonitrile. The concentration of BODIPY was 2 μM in each sample. The excitation wavelengths for BODIPY **1a–d** were at 520 nm, 540 nm, 530 nm, and 520 nm, respectively.

Figure 4. Change in the absorption (a) and fluorescence (b) spectra of BODIPY **1a** with increasing Cu^{2+} concentration in acetonitrile. The concentration of BODIPY **1a** was 2 μM. The excitation wavelength was 550 nm.

Figure 5. (a) Plot of the ratio of fluorescence peak intensities (F_{620}/F_{581}) of BODIPY **1a** versus

increasing Cu^{2+} concentration in acetonitrile. (b) Benesi–Hildebrand plot of absorbance at 502 nm.

Figure 6. Change in the ratio of fluorescence intensities (F_{620}/F_{581}) of BODIPY **1a** upon addition of various metal cations. The white bars represent the addition of each cation (10 μM). The black bars represent the subsequent addition of Cu^{2+} (10 μM).

Table 1. Synthetic yields (%) of BODIPY **1a–d**.

Product	1st step	2nd step
1a	75	80
1b	15	10
1c	12 % in the whole two steps[a]	
1d	96	24

[a] The crude solid obtained in the 1st step was used for the subsequent 2nd step because we could not separate monophenyl- and diphenyl-substituted BODIPY.

Table 2. Spectroscopic and photophysical properties of BODIPY **1a–d** in acetonitrile.

BODIPY	λ_{abs} (nm)	λ_{flu} (nm)	ε ($M^{-1}cm^{-1}$)	Φ	Stokes shifts (cm^{-1})
1a	502	581	28000	0.63	2700
1b	524	599	27000	0.58	2400
1c	509	582	30000	0.62	2500
1d	534	560	18000	0.63	900

Table 3. Spectroscopic and photophysical properties of BODIPY **1a–d** (2 μM) with Zn^{2+} (200 μM) in acetonitrile. $\Delta\lambda$ is the extent of the shift in wavelength caused by the addition of Zn^{2+}.

BODIPY	λ_{abs} (nm)	λ_{flu} (nm)	$\Delta\lambda_{abs}$ (nm)	$\Delta\lambda_{flu}$ (nm)	ε (M^{-1} cm^{-1})	Φ
1a	542	570	40	-11	41000	0.84
1b	559	590	35	-9	44000	0.59
1c	543	569	34	-13	48000	0.74
1d	506	536	-28	-24	14000	1.00

Table 4. Spectroscopic and photophysical properties of BODIPY **1a–d** (2 μM) with Cu^{2+} (200 μM) in acetonitrile. $\Delta\lambda$ is the extent of the shift in wavelength caused by the addition of Cu^{2+}.

BODIPY	λ_{abs} (nm)	λ_{flu} (nm)	$\Delta\lambda_{abs}$ (nm)	$\Delta\lambda_{flu}$ (nm)	ε ($M^{-1}cm^{-1}$)	Φ
1a	590	620	88	39	47000	0.28
1b	604	647	80	48	38000	0.03
1c	588	619	79	37	42000	0.16
1d	504	535	-30	-25	8000	0.23

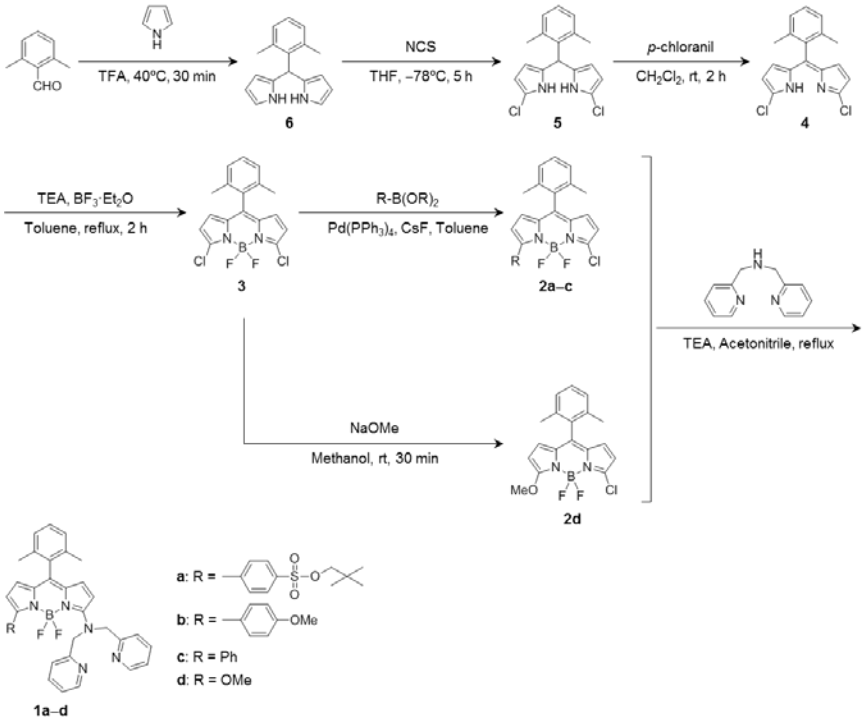

Scheme 1. Synthesis of BODIPY **1a–d**.

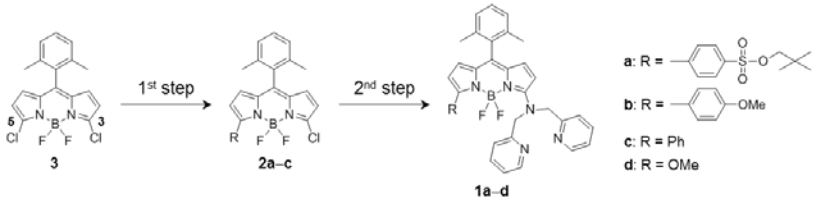

Figure 1. Synthetic route and the chemical structures of BODIPY **1a–d**.

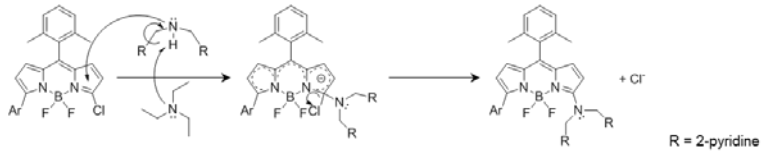

Figure 2. Possible reaction mechanism for the aromatic nucleophilic substitution of 5-aryl-BODIPY.

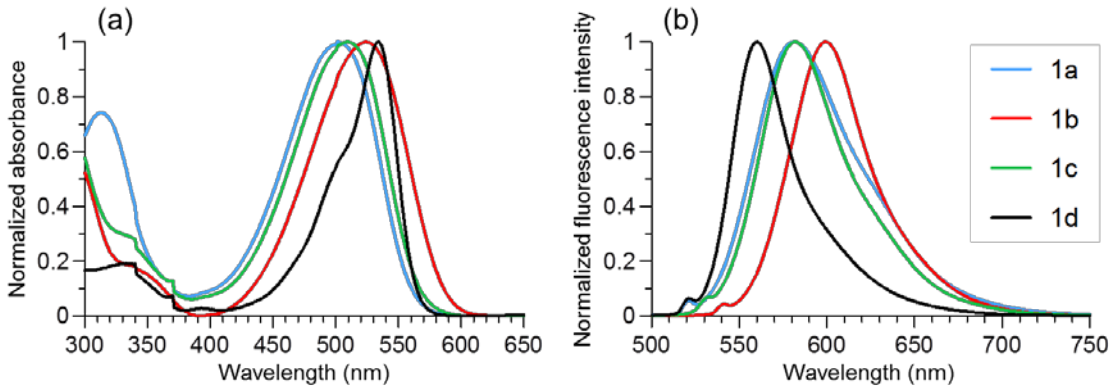

Figure 3. Normalized absorption (a) and fluorescence (b) spectra of BODIPY **1a–d** in acetonitrile. The concentration of BODIPY was 2 μM in each sample. The excitation wavelengths for BODIPY **1a–d** were at 520 nm, 540 nm, 530 nm, and 520 nm, respectively.

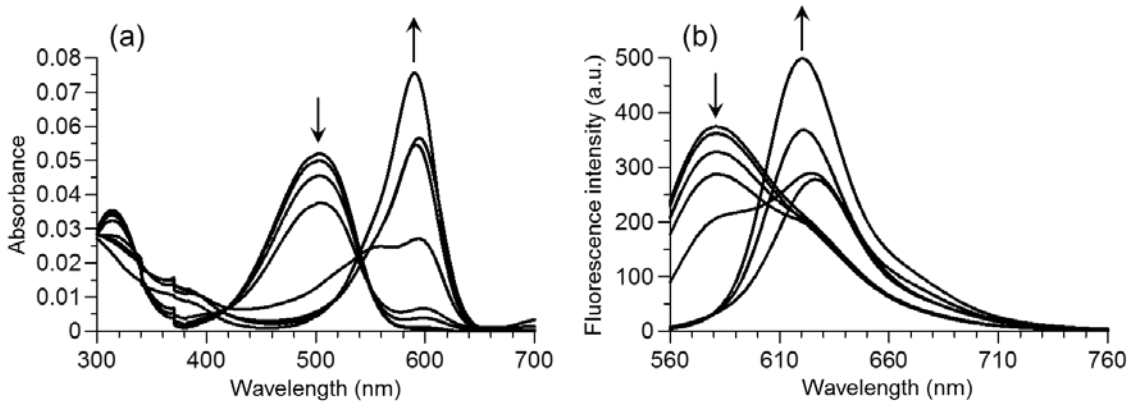

Figure 4. Change in the absorption (a) and fluorescence (b) spectra of BODIPY **1a** with increasing Cu^{2+} concentration in acetonitrile. The concentration of BODIPY **1a** was 2 μM. The excitation wavelength was 550 nm.

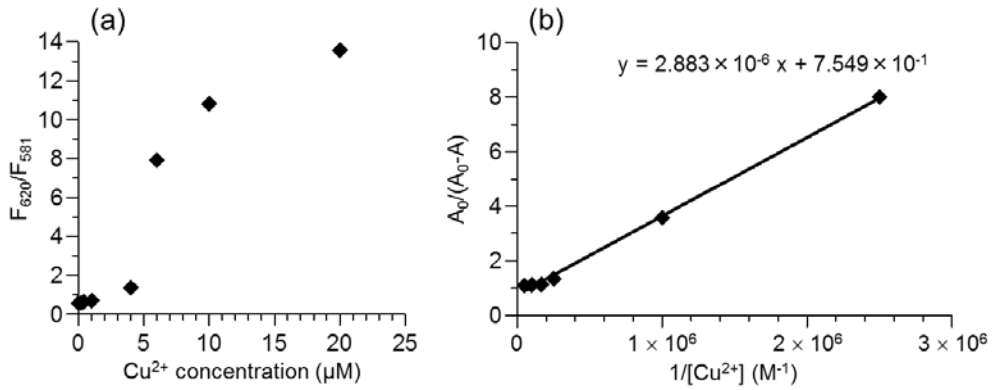

Figure 5. (a) Plot of the ratio of fluorescence peak intensities (F_{620}/F_{581}) of BODIPY **1a** versus increasing Cu^{2+} concentration in acetonitrile. (b) Benesi–Hildebrand plot of absorbance at 502 nm.

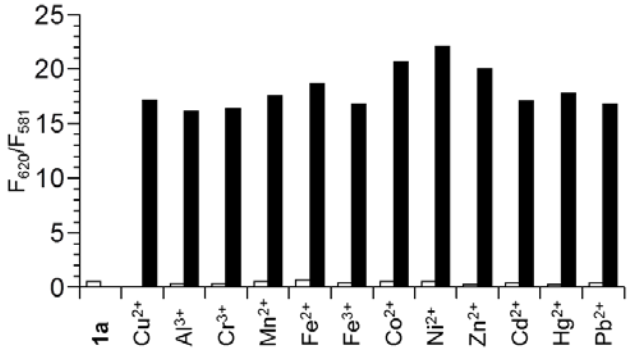

Figure 6. Change in the ratio of fluorescence intensities (F_{620}/F_{581}) of BODIPY **1a** upon addition of various metal cations. The white bars represent the addition of each cation (10 μM). The black bars represent the subsequent addition of Cu^{2+} (10 μM).

Substituent effects at the 5-position of 3-[bis(pyridine-2-ylmethyl)amino]-BODIPY cation sensor used for ratiometric quantification of Cu^{2+}

Akira Hafuka,* Ryosuke Kando, Kohei Ohya, Koji Yamada, Satoshi Okabe, and Hisashi Satoh

We investigated the effects of substitution at the 5-position of an asymmetric BODIPY cation sensor. Substituent groups with differing electron density were introduced at the 5-position. The sulfonylphenyl-substituted BODIPY showed high fluorescence quantum yield and ratiometric spectral change for Cu^{2+}.